RESEARCH ARTICLE

Cytotoxicity of Mitomycin C-Porous Silicon in Human Prostate Carcinoma Cells

Sazan M. Haidary[1,4], Nihad K. Ali[2*], Kosar A. Omer[1], Fadzilah A. Abdul Majid[3], Emma P. Córcoles[1], Malarvili M. B.[1]

[1]*Faculty of Biosciences and Medical Engineering (FBME), Universiti Teknologi Malaysia, 81310 Skudai, Johor, Malaysia.*
[2]*Department of Medical Physics, Faculty of Science, Al-Karkh University of Science, Baghdad, Iraq.*
[3]*Institute of Bioproducts Development, Faculty of Chemical Engineering, Universiti Teknologi, Malaysia, 81310 Skudai, Johor, Malaysia*
[4]*Food technology department, Faculty of Agriculture Engineering Science, Salahaddin University, Erbil, Iraq*

Received: 23rd March, 2020; Revised: 19th April, 2020; Accepted: 29th May, 2020; Available Online: 25th June, 2020

ABSTRACT

Porous silicon (pSi) microparticles with pore diameter 15 to 20 nm were fabricated by electrochemical etching of single-crystalline silicon (Si) wafers (n-type) to be used as delivery systems for the anticancer drug mitomycin C (MMC). The *in vitro* toxicity of the mitomycin-loaded pSi carrier was investigated on human prostate carcinoma (DU145) cells. The cells showed a decrease in viability of ~80% over a 6 hours period, when using mitomycin. Meanwhile, a ~55% decrease in cell viability was observed, when using the pSi carrier to deliver the drug. The drug-loaded carrier showed a sustained release throughout 24 hours, with an 80% decrease in cell viability after 16 hours. This observed controlled release of mitomycin from the pSi carrier suggests a superior therapeutic effect than the direct administration of mitomycin, as it potentially minimizes the drug side effects. Results showed that the strong cytotoxic effect towards the prostate cancer cells was due to the drug and not the carrier since the mitomycin-loaded pSi carrier affected cell viability, but the pSi carrier showed no toxicity. Furthermore, it was observed that with a higher amount of drug-loaded carriers, the toxicity effect was higher, thus, allowing further control of the therapeutic effect of the carrier.

Keywords: Drug delivery, Mitomycin C, Porous Si, Prostate cancer.

International Journal of Drug Delivery Technology (2020); DOI: 10.25258/ijddt.10.2.14

How to cite this article: Haidary SM, Ali NK, Omer KA, Majid FAA, Córcoles EP, Malarvili MB. Cytotoxicity of mitomycin C-Porous silicon in human prostate carcinoma cells. International Journal of Drug Delivery Technology. 2020;10(2): 265-272.

Source of support: Nil.

Conflict of interest: None

INTRODUCTION

Advances in nanotechnology are playing an important role in medicine and therapeutic areas. It is evident in fields such as nanomedicine, where drugs are delivered utilizing degradation and self-regulation of the carrier as a result of the material properties. Nanoparticles are attractive chemotherapeutic devices, since they have the potential to increase drug levels within tumors by circumventing the tumor vasculature, while decreasing normal tissue toxicities by reducing the level of drug in the systemic circulation.

pSi is a well-known biodegradable and biocompatible material as it degrades in physiological fluids over a period of time into nontoxic orthosilicic acid [$Si(OH)_4$], which is the natural form of Si found in the body.[1] The pSi nanoparticles have been used in multiple applications, such as, cell culture,[2] optical biosensing, biomolecular screening, tissue engineering, and drug delivery.[3,4]

A simple fabrication of pSi by electrochemical etching of Si wafers in an electrolyte solution produces Si nanoparticles, whose pore size, porosity, and thickness can be easily controlled depending on various fabrication parameters.[5,6] pSi offers unique advantageous properties, such as, its high specific surface area (200-800 m^2/g). Furthermore, surface modification, by oxidation, hydrosilylation, or grafting techniques, increases pSi stability in aqueous solution, making it suitable for drug delivery.[7] Multiple studies have used loaded pSi particles for *in vitro* drug release.[8-10] The cytotoxicity of pSi microparticles in Caco-2 cells was demonstrated *in vitro* as a function of concentration, particle size fraction and incubation times,[11] and *in vivo* with the release of peptide and ghrelin.[12]

**Author for Correspondence: nihad@kus.edu.iq, n.k.alobaidi@gmail.com*

Other payloads, such as, proteins[13] and the anticancer drug doxorubicin[14] have also been investigated. Recently *in vitro* cytotoxicity of mitoxantrone dihydrochloride loaded pSi thin films was demonstrated on human breast carcinoma.[15] The biocompatibility of pSi has also been demonstrated in various studies, using implants of pSi in rat abdominal wall[16] or as a drug carrier in a mouse model.[17] Rosengren *et al.* showed the luminescent pSi nanoparticles self-destructed into renal cleared components in a relatively short period with no evidence of toxicity.[16] While in another study, pSi particles were suggested as ideal oral drug delivery devices due to their exhibited excellence *in vivo* stability, low cytotoxicity, and inflammatory responses in Caco-2 and RAW 264 cells.[18] More recently, methotrexate pSi nanoparticles were used as a conjugated platform for combination chemotherapy by concurrently enhancing the dissolution rate of a hydrophobic drug and sustaining the release of drugs.[19] While, two anticancer drugs, doxorubicin and paclitaxel, were separately loaded into the nanocomposite drug delivery prepared by coating pSi nanoparticles with poly(beta-amino ester) and pluronic F-127.[20]

MMC, a [6-amino-8a-methoxy-5-methyl-4,7-dioxo-1, 1a, 2, 4, 7, 8, 8a, 8b-octahydroazireno [2',3':3,4] pyrrolo [1, 2-a] indol-8-yl] methylcarbamate, is a bifunctional alkylating agent that acts as genotoxic antibiotic. MMC also acts as a DNA cross-linking agent, blocking DNA synthesis and inhibiting cell mitosis, which in turns detains the cell cycle. Hence, MMC has been broadly used as a chemotherapeutic agent for over 20 years.[21] Jones *et al.* published the first study about the investigation of mitomycin activity as a single agent in prostate cancer.[22] Since then, different types of cancers, such as, bladder cancer,[23] and resected gastric cancer,[24] among others, have been treated with MMC. Several studies have pointed to the toxic side effects of MMC and suggested treatment to reduce these undesirable effects.[25,26] However, avoiding or minimizing these side effects and improving drug efficacy and bioavailability can be accomplished by using drug delivery devices. Several methods have been investigated for the delivery of MMC in nano or micro size. Common methods for MMC delivery consist of encapsulation of the drug in nano- or micro-particles, using biodegradable polymers including albumin,[27] dextran,[28] estradiol,[29] N-succinyl-chitosan,[30] hydrogels,[31] polybutylcyanoacrylate,[32] poly-epsilon-caprolactone,[33] oxidized-dextran microspheres,[28] and polylactic acids (PLA) nanoparticles.[34] However, to our knowledge, MMC has never been loaded into pSi.

In the present study, nanostructured pSi was fabricated as a carrier for delivery of MMC, allowing for a better drug release profile that can potentially prevent the drug side effects. The MMC loading efficacy, release profile, and *in vitro* cytotoxicity on human prostate carcinoma (DU145) cells were studied and compared to the behavior of empty pSi. Empty and MMC-loaded carriers were characterized by field emission scanning electron microscopy (FESEM), spectroscopy, and FTIR.

MATERIALS AND METHODS

All chemicals, such as, hydrofluoric acid 49%, ethanol absolute 99.8%, ammonium hydroxide 28–30%, hydrochloric acid (AR, 35–37%), and hydrogen peroxide (30 wt.% in H_2O) were purchased from Sigma Aldrich, Malaysia. MMC (*Streptomyces caespitosus*) was from Sigma, Germany. Cell culture media, fetal bovine serum, Dulbecco's modified Eagle's medium (DMEM) high glucose, L-Glutamine with sodium pyruvate, and Dulbecco's phosphate buffer saline were purchased from Biowest (Nuaillé, France). Si wafers were obtained from Siltronix SAS (Archamps, France).

Fabrication and Characterization of pSi

pSi samples were prepared from single-crystalline n-type Si wafers. These were first cleaned as per RCA clean procedure, a standard set of wafer cleaning steps, to remove contaminants present on the surface of the wafer. The procedure has three major steps: 1) the removal of organic contaminants is performed with an alkaline solution of 1:1:5 NH_4OH:H_2O_2: H_2O for 10 minutes at 70–80ºC, 2) the removal of a thin oxide layer is carried out by immersion of the silicon wafer in a diluted hydrofluoric acid (1:50) solution for 15 seconds, 3) an acidic solution of (1:1:6) HCl:H_2O_2: H_2O for 10 minutes at 70-80ºC is used to remove ionic and heavy metals traces. The pSi samples were prepared through an electrochemical etching of the n-type Si wafer with resistivity 0.008–0.018 Ω cm and orientation (100) in a simple electrochemical Teflon cell, containing electrolyte solution of (1:4) hydrofluoric acid (49%) and ethanol (99.8%). The exposed area of the silicon wafer (0.5 cm^2) was in contact with the backside of the aluminum foil. A platinum spiral coil was used as the counter-electrode, and the etching was carried out at a current density of 20 mA/cm^2 for 30 minutes. The process was performed with the illumination of incandescent light set 15 cm away from the sample. Following the electrochemical etching, the pores were separated from the substrate by a lift-off method. Freestanding films were obtained by abruptly increasing the current density to 250 mA/cm^2. Samples were rinsed first with deionized water, and then in ethanol. The freestanding films were then converted into microparticles with an average size of 36.72 µm by using ultrasonic fracture for 10 minutes in absolute ethanol.

Following the etching procedure, the pSi nanoparticles are typically unstable in aqueous solution, a fact attributable to the oxidation of the reactive surface hydrides. Hence, hydrosilylation was used to enhance its stability. The freshly prepared pSi nanoparticles were then placed in a 10 mL Pyrex beaker and 1 mL of undecylenic acid (≥95%) was added. This solution was heated in a commercial consumer microwave oven at full power (800 watts) for 5 minutes, and the particle was then rinsed with ethanol to remove any excess undecylenic acid. This surface can resist corrosion in PBS solution, and exhibits a slower release rate than freshly prepared pSi, which is unstable in aqueous solutions at pH 7.4.

The morphology of the pSi was characterized by field emission scanning electron microscopy (FESEM) using Zeiss

(supra 35vp JSM-6701F) instrument at an accelerated voltage of 1 keV. A Perkin Elmer TM 400 FTIR spectrometer (Waltham MA USA) was used to investigate the chemical bonds. The samples for Fourier transforms infrared spectroscopy (FTIR) analysis were prepared by grounding the sample with KBr and pressing it into a mold. The silicon carrier were degassed at 130°C for 1-hour prior to the Nitrogen adsorption-desorption measurements. These were carried out at a temperature of 130°C to determine the specific surface area of the Si nanoparticles using a gas composition of 30% N_2 and 70%, and calculated using the Brunauer Emmett Teller (BET) model.

Cell Line Maintenance and Growth Assay

Human prostate carcinoma (DU145) cell line catalog number HTB-81 was purchased from ATCC, United States. The cell line was derived from a metastatic site in the brain of a 69 years old Caucasian male. It consists of adherence cells, which are shaped like epithelial cells. Full details are provided in the ATCC catalog of the cell line. According to the growth profile, the cell seeding was performed by taking the cells from the vials kept in liquid nitrogen and transferring them to a water bath at 37°C until completely thawed. The cells were then transferred into a centrifuge tube with 9 mL of DMEM medium supplemented with 1% (v/v) streptomycin, and 10% (v/v) fetal bovine serum. This mixture was spun for 10 minutes at 3,300 rpm. After centrifugation the supernatant was removed and the pellets were suspended with the recommended amount of the pre-warmed, complete DMEM and transferred to 75 cm^2 T-flask and incubated at 37°C in a humidified atmosphere of 5% CO_2. The cells were allowed to attach to the plastic surface of the flask until confluence by changing the medium every 48 hours. The supernatant from the culture was removed and the cells layer was washed with 10 mL of PBS (pre-warmed in a water bath at 37°C) and discarded, then replaced with the fresh complete DMEM medium. The medium replacement was carried out until the confluence of the cells.[35] All the methods were followed as per described in the DU145 cell line data sheet from ATCC. Once confluence occurred, cells were trypsinized to detach them from the surface and prepared for cell counting. The supernatant of confluence cells was discarded, and cells were washed with pre-warmed PBS. 0.5 mL of trypsin EDTA (0.25% trypsin, EDTA 4 Na) was added to the flask, ensuring that it covered the whole monolayer. The flask was kept horizontally and incubated for 5 minutes at 37°C, until the monolayers detached, and then the appropriate volume of pre-warmed complete media was added to the detached cells and mixed gently. The mixture was transferred to the centrifuge tube and spun at 3,300 rpm for 10 minutes. The medium was discarded, the pellets were resuspended with complete medium, and the cells were counted using the trypan blue method as described below.[35] Try pan blue exclusion test, using Neubauer improved bright-line hemocytometer (Hausser, USA) was used for cell counting. 20 µL of the cells suspension was mixed with 20 µL of try pan blue dye. The number of viable cells and dead cells (stained with blue dye) were counted under a light microscope.[35]

Sterilization of Porous Silicon and Drug Loading Procedure

pSi samples were sterilized with 75% ethanol for 30 minutes, and rinsed with sterile water prior to the loading of the drug.[36] The particles were immersed in an aqueous solution of MMC, and the solvent was allowed to evaporate, leaving the drug packed into the pores via spontaneous adsorption. The particles were rinsed with deionized water in order to remove the drug that had not infiltrated the pores, and hence, remained on the surface of the particles. Drug loading percentage was calculated by the following equation (eq. 1):

$$\text{Drug Loading}(\%) = \frac{\text{WT MMC} - \text{pSi}}{\text{WT pSi}} \times 100 \quad (1)$$

where,

WT MMC-pSi = Weight of MMC loaded pSi

WT pSi = Weight of pSi only

Cell Cytotoxicity Assay

Cell viability was assessed using cells incubated with pSi (negative control), MMC-loaded pSi, and free MMC (positive control) during a period from 2 to 24 hours. Try pan blue assay was used for quantitative analysis of cell viability in order to estimate the functional toxicity of the released MMC after an exposure period from 2 to 24 hours. Cell viability was determined from two independent experiments, in which duplicate measurements were performed for each sample. 1 mL of cells at a concentration of 2×10^5 cells/mL were loaded into each well of a 6 well plate and incubated for 24 hours. Three different samples were used in this experiment: 1) pSi (negative control) at a concentration of ~10 mg/mL, 2) MMC-loaded pSi consisting of 10 mg/ml of pSi loaded with 2.99×10^{-3} M (~0.3 mg/mL) of MMC, and 3) free MMC (positive control) at a concentration corresponding to the drug released after 24 hours (~0.3 mg/mL). 1 mL of each sample was added into its correspondent well plate. Test plates were incubated at 37°C in a humidified atmosphere of 5% CO_2 for a period of 24 hours. One test plate was measured for its viability at intervals of 2, 4, 6, 16, 18, 20 and 24 hours. All samples were prepared in duplicate.

The effect of the quantity of particles used when preparing MMC-loaded pSi on cell viability was also investigated using a similar method as above. First, 4 mg/mL of MMC were added into solutions containing 3.25, 6.5, 13, and 26 mg of pSi particles. 1 mL of cells at a concentration of 2×10^5 cells/mL was loaded into each well in a 6 well plate, as indicated in the ATCC catalog of the cell line. Cells were allowed to attach for 24 hours at 37°C in a humidified atmosphere of 5% CO_2. Then, 1 mL of each of the different MMC-loaded pSi solutions was added to each correspondent well, and incubated with the cells for another 24 hours. Each sample was prepared in duplicate. Cell viability was counted using trypan blue methods.

RESULTS AND DISCUSSION

pSi Fabrication and Characterization

The previously described anodization procedure was optimized to obtain a uniform pSi layer in terms of both pore size and

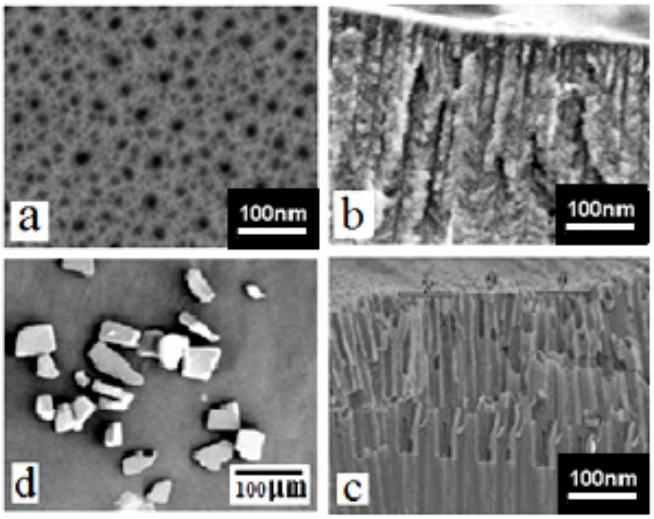

Figure 1: SEM images of porous silicon sample etched in HF: Ethanol, 1:4 by volume, applied current density of 20 mA/cm^2 for 30 minutes; (a) top view; (b) and (c) is a cross-section of the sample, before and after ultrasonic fracture, respectively; (d) porous silicon microparticles after sonication for 10 minutes

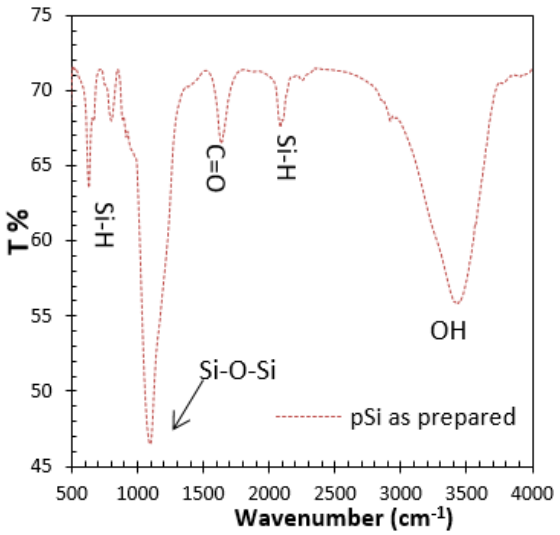

Figure 2: FTIR spectra of pSi prepared electrochemically in Teflon cell, containing electrolyte solution of (1:4) hydrofluoric acid (49%) and ethanol (99.8%).

pore distribution. The average pore diameter of 24.4 ± 8.5 nm was obtained, with a modal group of 15 - 20 nm (n = 130, SD).

The reproducibility of the structural features of pSi is an important issue. Hence, in this work we used the optimum experimental parameters [(1:4) volume ratios of 49% hydrofluoric acid and 99.8% ethanol anodizing solution, and a current density of 20 mA/cm^2 for 30 minutes] during pSi preparation to obtain the desired reproducibility. Figure 1(a) and (b) show the top view and cross-section of one pSi sample prepared with these optimized etching parameters. When looking at the morphology of pSi, one can see, on a basic level, a crystalline silicon matrix surrounding a network of empty holes. Figure 1(c), which illustrates the cross-section of pSi sample after ultrasonication, clearly shows that all the pores were clean and empty from the residual Si species. These empty pores allow for a drug to be loaded, and then released in physiological solutions based on the degradation rate of the material itself. This is the core idea for the design of a MMC delivery device for the treatment of tumor cells. In this case, the pSi morphology has some advantages since it presents a higher nanoporous exposed surface per unit of volume of the material. Moreover, considering that the free space inside the nanopores has to be loaded with a drug in liquid form, clean pores [observed in Figure 1(c)] ensure that it is easier to load the drug through capillary effect compared with the branched ones in Figure 1(b).

Following the fabrication of pSi substrate, a lift-off method was utilized for removing the porous layer from the Si substrate. This was attained with the application of 250 mA/cm^2 current density during 30 seconds. The freestanding films were ultrasonically fractured (10 minutes in ethanol) to produce particles ranging in size from 10 to 30 µm as shown in Figure 1(d). The particle porosity was determined by gravimetric measurement. 68.97% porosity was obtained by measuring the starting weight of the sample and the subsequent weight of the sample after etching, and after stripping the layer from the bulk. The specific surface area of pSi particles was measured according to Brunauer-Emmett-Teller (BET) theory, which is based on a multilayer adsorption extrapolation of the monolayer molecular adsorption Langmuir theory. This model provides the specific surface area of the material based on the physical adsorption isotherms of gas molecules on a solid surface.[37] The specific surface area of the pSi particles was 460 m^2/g, which is considered an appropriate area for loading MMC molecules into those particles.[37]

Mitomycin Loading into pSi Carriers

Simple physical adsorption was employed to load the MMC within freshly etched pSi microparticles. For this, the freshly etched pSi microparticles were immersed in a saturated MMC solution. After evaporation of the drug solution, the particles were washed with deionized water and the presence of MMC in the carriers was confirmed by comparing the FTIR spectra of pSi microparticles before and after loading. The spectrum of fresh pSi (Figure 2) displays bands characteristic of surface hydride species, with a band assigned to Si-Hx at 2,100 cm^{-1},[8,10] and shows absorption bands near 1056 and 826 cm^{-1} which are associated with Si–O–Si bridges. The absorbance observed at 631, and 813 cm^{-1} peaks are attributed to Si-Si, and different SiH_2 deformation modes.[38] The loading percentage of MMC within the silicon particles was calculated (as per eq. 1) to be 31.8%, which is in accordance with other works.[39] The FTIR spectrum of MMC, according to Z. Hou, *et al.*,[34] shows the characteristic absorption peaks of $-NH_2$ and $-NH$ groups at 3,269 and 3,317 cm^{-1}, respectively, and the carbonyl C=O stretching vibration peak at 1,725 cm^{-1}. The absorption peaks observed at 1,550, 1,447, 1,384 and 1,065 cm^{-1} were attributed to NH_2, C=C, C-N, C-O, respectively.

The spectrum of MMC-loaded pSi particles [Figure 3(a)] illustrates new peaks compared with that of the pSi only.

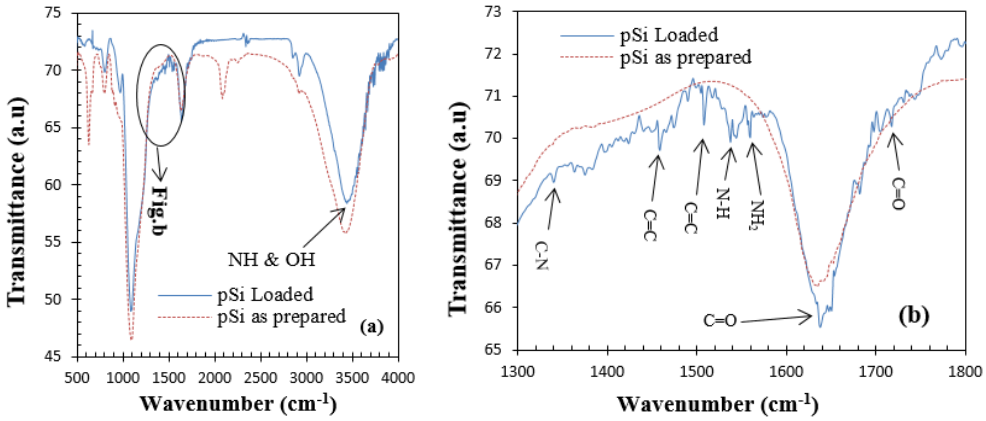

Figure 3: FTIR spectra **(a)** MMC-loaded pSi showing new peaks on the spectrum after MMC loading compared with freshly prepared pSi (dot line); **(b)** close-up of pSi and MMC-loaded pSi in the region from 1,300 to 1,800 cm^{-1}

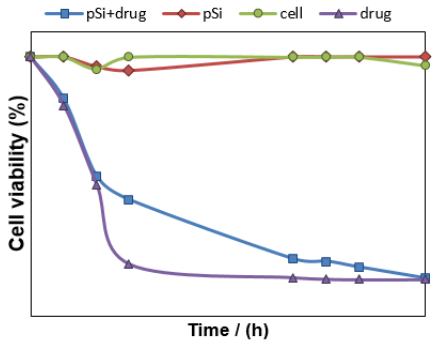

Figure 4: Viability of prostate cells after exposure of 2, 4, 6, 16, 18, 20 and 24 h to MMC-loaded pSi carriers (diamond symbols, blue trace), empty pSi (square symbols, red trace), negative control cell only (triangle symbols, green trace) and free MMC (cross symbol, purple trace).

The absorption bands were characterized and compared with other MMC FTIR analyses.[30,34,40] Broadband at 3,448 cm^{-1} was observed, which refers to the characteristic absorption peaks of the combination of OH, NH, and NH_2 groups. Peaks at 2,860 and 2,926 cm^{-1} correspond to the CH aromatic band, and the absorption bands at 1,000 to 1,250 cm^{-1} were assigned to C-O and Si-O. The area between 1,300 and 1,800 cm^{-1} was enlarged to identify the absorption peaks [Figure 3(b)]. The peaks at 1638 cm^{-1} correspond to amide II (–N-H) bending. The other absorption bands observed were at 1,335 cm^{-1} assigned to C-N stretching, at 1,560 cm^{-1} for the vibration bending of NH_2, at 1,508 cm^{-1} for the C=C aromatic, at 1,459 cm^{-1} for C=C stretching, and at 1,715 cm^{-1} for the carbonyl C=O stretching vibration.

In Vitro Cytotoxicity Assay

The human prostate Carcinoma cell line was used for cytotoxicity tests. Following growth profiles initially defined for each cell model, 2×10^5 cells were plated in each well of a 6-well plate. For analysis of cytotoxicity, cells were then exposed to MMC-loaded pSi carriers for a period between 2 to 24 hours at 37°C in 5% CO_2. At the end of each incubation (2 hours period),[14] cell viability was determined by measuring trypan blue exclusion, using the cell counters. Each experimental point was run in duplicate.

Figure 4 shows the cell viability percentage at intervals of 2 hours for 1) the prostate cells, 2) the cells with pSi carrier (negative control), 3) the cells with the MMC-loaded pSi carrier, and finally, 4) the cells with the MMC (positive control). The negative control was performed by incubating the Si particles with cells under the same conditions to prove that the pSi particles themselves did not cause the localized death of cells. This also allowed studying the effect of the carrier on the morphology of the cells.

From Figure 4, it can be observed that the MMC alone causes a decrease of cell viability of 80% within 6 hour, meanwhile, the drug-loaded into the pSi showed a more steady decrease, killing 80% of the cells only after 16 hours. The total viability of the cells in the positive control experiment (MMC alone) displays similar toxicity than pSi loaded with the drug, but the latter presents a controlled release of the drug; hence the toxicity time frame varies. By contrast, the negative control (empty pSi) showed no evident effect on cell viability; no dead cells were counted. The cells exposed to empty pSi carriers showed a 98.92 ± 2.02% viability, a result similar to that found in the case of cells alone 99.02 ± 1.83%, as observed in previous studies on other cell lines.[15,36] The morphology of the cell remained unchanged after the incubation with pSi, once more verifying that the localized cells' death was not caused by the pSi particles themselves.[41] This result was accepted as correct, since the cells had been carefully washed with PBS after removing the pSi and before adding the dye. This is a particularly important step when working with cell-based assays and pSi, due to the reaction of the dye with Si and silicic acid, its degradation product.[15] The cells' viability could be sorted from high to low as negative control (empty pSi) > pSi loaded with MMC > positive control (MMC). From these results, it can be concluded that the MMC released from freshly etched pSi particles displays significant toxicity towards the prostate cancer cells.

A series of experiments employing different amounts of MMC-loaded pSi carriers were incubated in separate well plates containing a similar quantity of prostate cancer cells. Figure 5 shows the percentage of dead cells *versus* the amount of MMC-loaded carrier incubated with the cells. When the drug

Table 1: Carriers used for the controlled delivery of MMC

Carrier	*Loading method*	*In vitro release medium*	*Monitoring of drug release*	*Cytotoxicity assay*	*Ref*
Conjugates of MMC with albumin-biodegradable macromolecular hybrid	MMC was covalently attached to the glutarylated bovine serum albumin	PBS (pH 7.4, 37 °C) and PBS-chymo-trypsin	Half-life ($t_{1/2}$) PBS = 155.3 hours $t_{1/2}$ PBS-chy = 24.5 hours	Intraperitoneal injection in mice inoculated with sarcoma 180	27
Oxidized sulfopropyl dextran microspheres	48 hours incubation of 1ml MMC at 4°C	0.15 M PBS (pH 7.4, 37 °C)	27% release after 48 hours by spectrophotometry and HPLC	Hemocytometer counter of EMT6 murine breast cancer cell	28
Conjugates of MMC with estradiol benzoate (EB) and estradiol (E) via glutaric acid (glu)-Suspension form	Synthesized by condensation of MMC with EB-glu and E-glu	Mixture of 1/15 M PBS & propylene glycol 9:1, v/v at 37 °C	Release after start of incubation: 2.7% EB-glu-MMC 35% E-glu-MMC by HPLC	Intraperitoneal administration in mice bearing P388 leukemia and sarcoma 180. Antitumor effect was measured comparing the survival time of treated and control mice.	29
N-succinyl-hydroxyethyl chitosan membrane (Suc-HECTS)	MMC cross-linked to Suc-HECTS butanedioldiglycidyl ether	PBS (pH 7.4, 37 °C)	Intensive release in the first 48 hours, t1/2 = 144 hours by ultravioletspectrophoto-metry	*In vitro* in L929 fibroblast cells *In vivo* subcutaneous tissue and skeletal muscle of Wistar rats by MTT assay	30
Hydrogels P (HEMA)	Redox polymerization method for loading MMC into 1% hydrogels	-	-	*In vitro* in COS-1 cells or human conjunctival fibroblasts. After 7 days in culture, cells nº in each dish were determined.	31
Polybutylcyanoacrylate nanoparticles (PBCA-NP)	PBCA monomer was added to a dextran 70 and MMC aqueous phase	-	-	CT scanning: In mice KM models MMC-PBCA-NP accumulated more in the liver compared to MMC. In rabbits bearing VX2 cells in the liver, both drugs had similar effects	32
Cationic nanoparticles: chitosan (CS), chitosan/ poly-ε-caprolactone (CS-PCL), poly-l-lysine/poly-ε-caprolactone(PLL-PCL)	MMC was dissolved (10% of polymer weight) in aqueous phase during nanoparticle preparation for encapsulation of drug in nanoparticles	Citrate buffer (pH 6.0)	Within 6 hours CS: 10% CS-PCL: 80% PLL-PCL: 20% by HPLC	MB49 bladder carcinoma cell line by MTT assay	33
Polylactic acid nanoparticles (PLA) and PLA with soybean phosphatidyl-choline (PLA-SPC)	MMC-SPC: anhydrous co-solvent lyophilization MMC-SPC-PLA: single emulsion solvent evaporation	PBS (pH 7.2, 37 °C)	Release over 30 days PLA-SPC: 50.17% PLA: 74.1% by UV/vis spectrometer at 365 nm	-	34
Phytosomes loaded with MMC-soybean phosphatidyl-choline (MMC-SPC)	Solvent evaporation method combined with a nanoprecipitation technique	PBS (0.02 M, pH 7.4) and 25% (v/v) mouse plasma	1 hour: 45.87% in PBS 50.57% in plasma 8 hours: 67.57% in PBS 69.34% in plasma by dynamic dialysis	*In vitro*: H22 cells determined by MTT assay, absorbance (570 nm) *In vivo*: Kunming mice inoculated subcutaneously with H22 cells by tumor inhibition rate *vs.* control group	40
Magnetic poly butyl cyanoacrylate nanoparticles	-	-	HPLC	Mouse plasma	42
pSi	Simple physical adsorption	Human prostate carcinoma cell line	Intensive release during first 6 hr until 24 hr by trypan blue exclusion measurement with cell counters	Human prostate carcinoma (DU145) Cell viability decreased to 20% within 16 hours for pSi compared to the 6 hours of MMC only bytrypan blue	This work

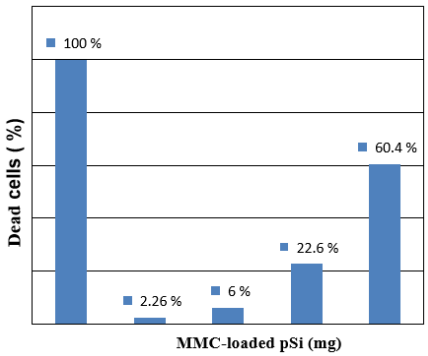

Figure 5: The percentage of dead cells *versus* the amount of MMC-loaded pSi carriers (based on loading efficacy) exposed to the cells

was incubated directly onto the cells, all the cells were observed dead (100%). Meanwhile, when the drug was loaded into the pSi carrier, much lower dead cells were observed. In this case, the quantity of dead cells was observed to increase with an increasing amount of particles. This can be explained due to the fact that higher amounts of particles contain higher amounts of drug load, as observed with other drugs-loaded pSi carriers.[41]

Other MMC Carriers

Other carriers have been used for the controlled delivery of MMC. The type of carrier, MMC-loading method, as well as the *in vitro* monitoring of the drug release and cytotoxicity assays have been described in Table 1.

While other carriers provide significantly long release times, such as, 155 hours[27] and 30 days,[34] due to the more elaborated drug loading method, either covalent attachment or by lyophilization, these might not be suitable for all types of anticancer treatments. In our work, simple physical adsorption was used to load the drug, and an important therapeutic effect was observed within 16 hours, an increase of 10 hours when using MMC-loaded pSi compared to the drug alone, in the human prostate carcinoma cells. The MMC carriers reported in the literature are based in hydrogels and polymeric particles in general, and have been used to show the therapeutic effect of these on sarcoma, leukemia, bladder, and breast cancer particularly. Considering the intrinsic properties of pSi (nontoxic, biodegradable, and photoluminescence) and hence, its position at the forefront of delivery devices, it is important to study this material individually for different drugs and applications. In light of this, this study has attempted to show the feasibility of using pSi as a MMC carrier for human prostate carcinoma treatment.

CONCLUSION

We have successfully fabricated pSi carriers with adequate pore sizes (15–20 nm) for the loading and controlled release of mitomycin, an anticancer agent with antibiotic activity used for the treatment of prostate cancer. The feasibility of MMC-loaded pSi particles as a chemotherapeutic device was investigated *in vitro* in a cytotoxicity study on human prostate carcinoma (DU145) cells. The MMC-loaded pSi carriers showed the same level of toxicity as the anticancer drug, but 10 hours later. These results suggest that pSi particles provide a more controlled release compared to the common drug administration method, where a rapid burst was observed only 6 hours after the MMC was added to the cell line. Further, no toxic effect was observed due to the pSi particles. The use of the carriers not only avoids an undesired burst effect, but allows for a more controlled release profile of the drug over an extended period. Additional toxicity was obtained by increasing the amount of drug-loaded particles, hence, increasing the effect of the carrier.

Further control can be attained by coating the particles or by surface modification. In addition, pSi is a known biodegradable material with photoluminescence properties, and thus, its elimination can be monitored via fluorescence microscopy. The controlled release of MMC via pSi carrier has the potential to improve the therapeutic effect of the drug and minimize its side effects by delivering a more precise dose on the tumor site. This work sheds more light on the use of pSi as a regional chemotherapy agent for the treatment of prostate cancer.

ACKNOWLEDGMENTS

The authors acknowledge the support of the Malaysian Ministry of Science, Technology, and Innovation (MOSTI) and Universiti Teknologi Malaysia (UTM) through vote no R.J130000.7945.4S107. The authors would like to thank PhD students Hala Abdulkareem and Shamsiah Muhamad for their valuable help and advice, as well as, the technicians of the TCEL lab in the Faculty of Chemical Engineering, where the *in vitro* study was conducted.

REFERENCES

1. Reffitt DM, Jugdaohsingh R, Thompson RPH, Powell JJ. Silicic acid: Its gastrointestinal uptake and urinary excretion in man and effects on aluminium excretion. Journal of Inorganic Biochemistry. 1999;76:141-147.
2. Baca HK, Ashley C, Carnes E, Lopez D, Hemming J, Dunphy D, *et al*. Cell-directed assembly of lipid-silica nanostructures providing extended cell viability. Science. 2006;313:337-341.
3. Haidary SM, Córcoles EP, Ali NK. Nanoporous Silicon as Drug Delivery Systems for Cancer Therapies. Journal of Nanomaterials 2012:1-15.
4. Santos HA, Mäkilä E, Airaksinen J, Bimbo M, Hirvonen J. Porous silicon nanoparticles for nanomedicine: preparation and biomedical applications.Nanomedicine. 2014;9:535-554.
5. Hirvonen J, Laaksonen T, Peltonen L, Santos H, Lehto V, Heikkilä T, *et al*. Feasibility of silicon-based mesoporous materials for oral drug delivery applications. Dosis. 2008;24:129-149.
6. Salonen J, Kaukonen AM, Hirvonen J, Lehto V. Mesoporous silicon in drug delivery applications. Journal of Pharmaceutical Sciences. 2008;97:632-653.
7. Anglin EJ, Cheng L, Freeman WR, Sailor MJ. Porous silicon in drug delivery devices and materials. Advanced Drug Delivery Reviews. 2008;60:1266-1277.
8. Anglin EJ, Schwartz MP, Ng VP, Perelman LA, Sailor MJ. Engineering the chemistry and nanostructure of porous silicon fabry-pérot films for loading and release of a steroid. Langmuir. 2004;20:11264-11269.

9. Salonen J, Laitinen L, Kaukonen AM, Tuura J, Björkqvist M, Heikkilä T, *et al*. Mesoporous silicon microparticles for oral drug delivery: Loading and release of five model drugs. Journal of Controlled Release. 2005;108:362-374.
10. Haidary SM, Córcoles EP, Ali NK. Folic acid delivery device based on porous silicon nanoparticles synthesized by electrochemical etching. International Journal of Electrochemical Science. 2013;8:9956-9966.
11. Santos HA, Riikonen J, Salonen J, Mäkilä E, Heikkilä T, Laaksonen T, *et al*. *In vitro* cytotoxicity of porous silicon microparticles: Effect of the particle concentration, surface chemistry and size. Acta Biomaterialia. 2010;6:2721-2731.
12. Kilpeläinen M, Riikonen J, Vlasova MA, Huotari A, Lehto VP, Salonen J, *et al*. Preparation and properties of a drug release membrane of mitomycin C with N-succinyl-hydroxyethyl chitosan. Journal of Controlled Release. 2009;137:166-170.
13. Pastor E, Matveeva E, Valle-Gallego A, Goycoolea FM, Garcia-Fuentes M. Protein delivery based on uncoated and chitosan-coated mesoporous silicon microparticles. Colloids and Surfaces B: Biointerfaces. 2011;88:601-609.
14. Vaccari L, Canton D, Zaffaroni N, Villa R, Tormen M, di Fabrizio E. Porous silicon as drug carrier for controlled delivery of doxorubicin anticancer agent. Microelectronic Engineering 2006;83:1598-1601.
15. Tzur-Balter A, Gilert A, Massad-Ivanir N, Segal E. Engineering porous silicon nanostructures as tunable carriers for mitoxantrone dihydrochloride. Acta Biomaterialia. 2013;9:6208-6217.
16. Rosengren A, Wallman L, Bengtsson M, Laurell T, Danielsen N, Bjursten L Tissue reactions to porous silicon: A comparative biomaterial study. Physica status solidi (a). 2000;182:527-531.
17. Park J-H, Gu L, von Maltzahn G, Ruoslahti E, Bhatia SN, Sailor MJ. Biodegradable luminescent porous silicon nanoparticles for *in vivo* applications. Nat Mater. 2009;8:331-336.
18. Bimbo LM, Sarparanta M, Santos HA, Airaksinen AJ, Makila E, Laaksonen T, *et al*. Biocompatibility of thermally hydrocarbonized porous silicon nanoparticles and their biodistribution in rats. ACS nano. 2010;4:3023-3032.
19. Wang C-F, Mäkilä EM, Kaasalainen MH, Hagström MV, Salonen JJ, Hirvonen JT. *et al*. Dual-drug delivery by porous silicon nanoparticles for improved cellular uptake, sustained release, and combination therapy. Acta Biomaterialia. 2015;16:206-214.
20. Xu W, Thapa R, Liu D, Nissinen T, Granroth S, Närvänen A. *et al*. Smart porous silicon nanoparticles with polymeric coatings for sequential combination therapy. Molecular Pharmaceutics. 2015;12:4038-4047.
21. Rauth AM, Mohindra JK, Tannock IF. Activity of mitomycin C for aerobic and hypoxic cells *in vitro* and *in vivo*. Cancer Research. 1983;43:4154-4158.
22. Jones WG, Foss SD, Bono AV, Croles JJ, Stoter G, Pauw Md, Sylvester R. Mitomycin-C in the Ireatment of metastatic prostate cancer: report on an EORTC phase H study. The Journal of Urology. 1986;4:182-186.
23. Tolley DA, Parmar MKB, Grigor KM, Lallemand G. The Effect of Intravesical Mitomycin C on Recurrence of Newly Diagnosed Superficial Bladder Cancer: A Further Report with 7 Years of Followup. The Journal of Urology. 1996;155:1233-1238.
24. Grau JJ, Estape J, Alcobendas F, Pera C, Daniels M, Teres J. Positive results of adjuvant mitomycin-C in resected gastric cancer: A randomised trial on 134 patients. European Journal of Cancer Part A: General Topics. 1993;29:340-342.
25. Ishiki N, Onishi H, MacHida Y. Evaluation of antitumor and toxic side effects of mitomycin C-estradiol conjugates. International Journal of Pharmaceutics. 2004;279:81-93.
26. Verweij J, van der Burg MEL, Pinedo HM. Mitomycin C-induced hemolytic uremic syndrome. Six casereports and review of the literature on renal, pulmonary and cardiac side effects of the drug. Radiotherapy and Oncology. 1987;8:33-41.
27. Tanaka T, Kaneo Y, Miyashita M, Shiramoto S. Properties of water-insoluble mitomycin C-albumin conjugate as a sustained release drug delivery system in mice inoculated with sarcoma 180. Biological and Pharmaceutical Bulletin. 1995;18:1724-1728.
28. Cheung RY, Ying Y, Rauth AM, Marcon N, Wu XY. Biodegradable dextran-based microspheres for delivery of anticancer drug mitomycin C. Biomaterials. 2005;26:5375-5385.
29. Ishiki N, Onishi H, Machida Y. Antitumor activities of conjugates of mitomycin C with estradiol benzoate and estradiol via glutaric acid in suspension dosage form. Biological and Pharmaceutical Bulletin. 2002;25:1373-1377.
30. Li M, Han B, Liu W. Preparation and properties of a drug release membrane of mitomycin C with N-succinyl-hydroxyethyl chitosan. J Mater Sci Mater Med. 2011;22:2745-2755.
31. Blake DA, Sahiner N, John VT, Clinton AD, Galler KE, Walsh M. *et al*. Inhibition of cell proliferation by mitomycin C incorporated into P(HEMA) hydrogels. J Glaucoma. 2006;15:291-298.
32. Xi-xiao Y, Jan-hai C, Shi-ting L, Dan G, Xv-xin Z. Polybutylcyanoacrylate nanoparticles as a carrier for mitomycin C in rabbits bearing VX2-liver tumor. Regulatory Toxicology and Pharmacology. 2006 Dec 1;46(3):211-7.
33. Bilensoy E, Sarisozen C, Esendağlı G, Doğan AL, Aktaş Y, Şen M, Mungan NA. Intravesical cationic nanoparticles of chitosan and polycaprolactone for the delivery of Mitomycin C to bladder tumors. International journal of pharmaceutics. 2009 Apr 17;371(1-2):170-176.
34. Hou Z, Wei H, Wang Q, Sun Q, Zhou C, Zhan C. *et al*. Phytosomes Loaded with Mitomycin C–Soybean Phosphatidylcholine Complex Developed for Drug Delivery. Nanoscale Research Letters. 2009;4:732-737.
35. Freshney RI. Culture of Specific Cell Types, in: Culture of Animal Cells, John Wiley & Sons, Inc., 2005.
36. Alvarez SD, Derfus AM, Schwartz MP, Bhatia SN, Sailor MJ. The compatibility of hepatocytes with chemically modified porous silicon with reference to *in vitro* biosensors. Biomaterials. 2009;30:26-34.
37. Brunauer S, Emmett PH, Teller E. Adsorption of Gases in Multimolecular Layers. Journal of the American Chemical Society. 1938;60:309-319.
38. Gupta P, Colvin V, George S. Hydrogen desorption kinetics from monohydride and dihydride species on silicon surfaces. Physical Review B. 1988;37:8234.
39. Perelman LA, Pacholski C, Li YY, VanNieuwenhz MS, Sailor MJ. pH-triggered release of vancomycin from protein-capped porous silicon films. Nanomedicine. 2008;3:31-43.
40. Hou Z, Li Y, Huang Y, Zhou C, Lin J, Wang Y, Cui F. *et al*. Phytosomes Loaded with Mitomycin C–Soybean Phosphatidylcholine Complex Developed for Drug Delivery. Molecular pharmaceutics. 2012;10:90-101.
41. Gu L, Park JH, Duong KH, Ruoslahti E, Sailor MJ, Magnetic luminescent porous silicon microparticles for localized delivery of molecular drug payloads. Small. 2010;6:2546-2552.
42. Liu W, Chen JH, Ren F, Guo YB, Yan XQ, Liu YD. Determination of magnetic mitomycin C-polybutylcyanoacrylate nanoparticles in mouse plasma Academic journal of the first medical college of PLA. 2005;25:413-415.